arXiv:1701.02273v2 [cs.CV] 31 Mar 2017

Visual Multi-Object Tracking for Unknown Clutter Rate

Du Yong Kim

Department of Electrical and Computer Engineering, Curtin University, Bentley, 6102

Abstract

In most multi-object tracking algorithms, tuning of model parameters is of critical importance for reliable performance. In particular, we are interested in designing a robust tracking algorithm that is able to handle unknown false measurement rate. The proposed algorithm is based on coupling of two random finite set filters that share tracking parameters. Performance evaluation with visual surveillance and cell microscopy images demonstrates the effectiveness of the tracking algorithm for real-world scenarios.

Keywords: Multi-object tracking, Visual tracking, random finite sets

1. Introduction

Multi-object tracking is one of fundamental problems in many applications. There are abundant research works, however, it is still far from practical use. The overwhelming majority of multi-target tracking algorithms are built on the assumption that multi-object system model parameters are known a priori, which is generally not the case in practice [1]. While tracking performance is generally tolerant to mismatches in the dynamic and measurement noise, the same cannot be said about missed detections and false detections. In particular, mismatches in the specification of false detection model parameters such as clutter intensity can lead to a significant bias or even erroneous estimates [2].

Unfortunately, except for a few application areas, exact knowledge of model parameters is not available. This is especially true in visual tracking, in which the missed detection and false detection processes vary with the detection methods. The clutter intensity model can be obtained by trial and error. A major problem is the time-varying nature of false detection processes. Consequently, there is no guarantee that the model

parameters chosen from training data will be sufficient for the multi-object filter at subsequent frames.

Stochastic multi-object tracking algorithms based on Kalman filtering or Sequential Monte Carlo (SMC) method have been widely used including visual multi-object tracking research [3], [4] where detection profile and false measurement rate are assumed to be known. On the other hand, deterministic approach such as network flow [5], continuous energy optimisation [6], has become a popular method for visual multi-object tracking problem. This approach is known to be free from measurement model parameters, however, it requires other user-specified parameters and is useful only when reliable object detection is available with negligible false measurements.

Unknown observation model parameters (i.e., clutter rate, detection profile) in online multi-object filtering was recently formulated in a joint estimation framework using random finite set (RFS) approach [1]. Recently, Mahler [2] showed that clever use of the CPHD filter can accommodate unknown clutter rate and detection profile. [7] extended it to multi-Bernoulli filter with SMC implementation. While the solution for filtering with unknown clutter rate exists, these filters do not provide tracks that identify different objects. To the best of our knowledge this paper is the first attempt for handling unknown false measurement information in online tracking with trajectories. The main contribution of this paper is to design a multi-object tracker that produces trajectories of individual objects and estimates unknown clutter rate on the fly.

2. Problem Formulation

Let $\mathbb{X} = \mathbb{R}^{n_x}$ denote the space of the target kinematic state, and $\{0, 1\}$ denote the discrete space of labels for clutter model and actual targets. Then, the augmented state space is given by $\breve{\mathbb{X}} = \mathbb{X} \times \{0, 1\}$, where $\times$ denotes a Cartesian product. Consequently, the state variable contains the kinematic state, and target/clutter indicator. We follow the convention from [7] that the label $u = 0$ will be used as a subscript to denote the clutter generators and the label $u = 1$ for actual targets.

Suppose that there are T_k target and clutter object, and we have O_k observations (i.e., detections). In the RFS framework, the collections of targets (including clutter

objects) and measurements can be described as finite subsets of the state and observation spaces, respectively as $\breve{X}_k = \{\breve{x}_{k,i}\}_{i=1}^{T_k} \subset \breve{\mathbb{X}}, \quad Z_k = \{z_{k,j}\}_{j=1}^{O_k} \subset \mathbb{Z}$, where $\breve{x}_{k,i}$ represent either the kinematic state of actual target or clutter target; $z_{k,j}$ is a measurement, and $\mathbb{Z}$ is the space of measurement, respectively.

Considering the dynamic of the state, the RFS model of the multi-target state at time k consists of surviving targets and new targets entering in the scene. This new set is represented as the union

$$\breve{X}_k = \bigcup_{\breve{x}_{k-1} \in \breve{X}_{k-1}} S_{k|k-1}(\breve{x}_{k-1}) \bigcup \Gamma_k, \tag{1}$$

where Γ_k is a set of spontaneous birth objects (actual or clutter targets) and $S_{k|k-1}(\cdot)$ is the set of survived object states at time k with survival probability $p_S(\breve{x}) < 1$.

The set of observations given the multi-target state is expressed as

$$Z_k = Z_{T,0,k} \bigcup Z_{T,1,k}, \tag{2}$$

where $Z_{T,0,k}$ and $Z_{T,1,k}$ are, respectively, sets of clutter and target-originated observations with unknown detection probability $p_D(\breve{x}) < 1$.

With the RFS multi-target dynamic and measurement model, the multi-object filtering problem amounts to propagating multi-target posterior density recursively forward in time via the Bayes recursion. Note that in the classical solution to this filtering problem such as PHD, CPHD [1], and multi-Bernoulli filters [4], instead of clutter target measurement set, the Poisson clutter intensity is given and the detection profile $p_D(x)$ is also known a priori [1].

3. Multi-object tracker with unknown clutter rate

The aim of this paper is to propose a new online multi-object tracker that is able to accommodate unknown clutter rate. For this purpose, the Robust Multi-Bernoulli (RMB) filter [7] is employed to adapt unknown clutter rate. Then, the RMB filter is coupled with the Generalized Multi-Bernoulli (GLMB) tracker [8] by exchanging parameters to achieve robust performance as will be given in Section 4.

3.1. Robust Multi-Bernoulli Filter

The multi- Bernoulli filter parametrizes the multi-object posterior density by using a set of pairs, i.e., Bernoulli parameters, $\{(r^{(i)}, p^{(i))}\}_{i=1}^{M}$ where $r^{(i)}$ and $p^{(i)}$ represent the existence probability and the density of the state among M Bernoulli components. The multi-Bernoulli filter recursion for extended state space called RMB filter [7] is summarized to make the paper self-contained.

If the posterior multi-object density of the multi-Bernoulli form at time $k-1$ is given as $\{(r_{k-1}^{(i)}, p_{u,k-1}^{(i)})\}_{i=1}^{M_{k-1}}$. Then, the predicted intensity is approximated by a set of following multi-Bernoulli components $\{(r_{k|k-1}^{(i)}, p_{u,k|k-1}^{(i)})\}_{i=1}^{M_{k|k-1}}$. A set of predicted Bernoulli components is a union of birth components and surviving components. The birth Bernoulli components, $\{(r_{\Gamma,k}^{(i)}, p_{\Gamma,u,k}^{(i)})\}_{i=1}^{M_{\Gamma,k}}$, are chosen a priori by considering the entrance region of the visual scene, e.g., image border. The surviving components are calculated by

$$r_{P,k|k-1}^{(i)} = r_{k-1}^{(i)} \sum_{u=0,1} \langle p_{u,k-1}^{(i)}, p_{S,u,k} \rangle, \;\; p_{u,k|k-1}^{(i)}(x) = \frac{\left\langle f_{u,k|k-1}(\breve{x}|\cdot,) p_{u,k-1}^{(i)}, p_{S,u,k} \right\rangle}{\left\langle p_{u,k-1}^{(i)}, p_{S,u,k} \right\rangle}, \tag{3}$$

where $p_{S,u,k}$ is the survival probability to time k and $f_{u,k|k-1}(\breve{x}|\cdot)$ is the state transition density specified by either for actual target or for clutters as denoted by u.

If at time k, the predicted multi-target density is multi-Bernoulli form, then the updated multi-Bernoulli density approximation is composed of the legacy components with the subscript L and the measurement updated components with the subscript U as $\{(r_{L,k}^{(i)}, p_{L,u,k}^{(i)})\}_{i=1}^{M_{k|k-1}} \cup \{(r_{U,k}(z), p_{U,u,k}(\cdot; z))\}_{z \in Z_k}$. The legacy and measurements updated components are calculated by a series of equations (4) as follows.

$$\begin{aligned}
&r_{L,k}^{(i)} = \textstyle\sum_{u=0,1} r_{L,u,k}^{(i)}, \quad r_{L,u,k}^{(i)} = \frac{r_{k|k-1}^{(i)} \left\langle p_{u,k|k-1}^{(i)}, 1-p_{D,u,k} \right\rangle}{1-r_{k|k-1}^{(i)} \sum_{u'=0,1} \left\langle p_{u',k|k-1}^{(i)}, p_{D,u',k} \right\rangle}, \\
&p_{L,u,k}^{(i)}(x) = \frac{\left(1-p_{D,u,k}\right) p_{u,k|k-1}^{(i)}(x)}{\sum_{u'=0,1} \left\langle p_{u',k|k-1}^{(i)}, 1-p_{D,u',k} \right\rangle}, \quad r_{U,k}(z) = \textstyle\sum_{u=0,1} r_{U,u,k}(z), \\
&r_{U,u,k}(z) = \frac{\sum_{i=1}^{M_{k|k-1}} \frac{r_{k|k-1}^{(i)} \left(1-r_{k|k-1}^{(i)}\right) \left\langle p_{u,k|k-1}^{(i)}, g_{u,k}(z,|\cdot) p_{D,u,k} \right\rangle}{\left(1-r_{k|k-1}^{(i)} \sum_{u'=0,1} \left\langle p_{u'=0,1}^{(i)}, p_{D,u',k} \right\rangle\right)^2}}{\sum_{i=1}^{M_{k|k-1}} \frac{r_{k|k-1}^{(i)} \sum_{u'=0,1} \left\langle p_{u,k|k-1}^{(i)}, g_{u',k}(z|\cdot) p_{D,u',k} \right\rangle}{1-r_{k|k-1}^{(i)} \sum_{u'=0,1} \left\langle p_{u',k|k-1}^{(i)}, p_{D,u',k} \right\rangle}}, \\
&p_{U,u,k}(x; z) = \frac{\sum_{i=1}^{M_{k|k-1}} \frac{r_{k|k-1}^{(i)}}{1-r_{k|k-1}^{(i)}} p_{u,k|k-1}^{(i)}(x) g_{u,k}(z|x) \cdot p_{D,u,k}}{\sum_{u'=0,1} \sum_{i=1}^{M_{k|k-1}} \frac{r_{k|k-1}^{(i)}}{1-r_{k|k-1}^{(i)}} \left\langle p_{u',k|k-1}^{(i)}, g_{u',k}(z|\cdot) p_{D,u',k} \right\rangle}
\end{aligned} \tag{4}$$

where $p_{D,u,k}$ is the state dependent detection probability, $g_{u,k}(z|x)$ is the measurement likelihood function that will be defined in the following section. Note that the implementation details can be found in [7].

3.2. Generalized labeled Multi-Bernoulli Filter

The generalized labeled multi-Bernoulli (GLMB) filter provides a solution of multi-object Bayes filter with unique labels [8]. In multi-object tracking with labels, formally, the state of an object at time k is defined as $\mathbf{x}_k = (x_k, \ell_k) \in \mathbb{X} \times \mathbb{L}_k$, where $\mathbb{L}_k$ denotes the label space for objects at time k (including those born prior to k). Note that $\mathbb{L}_k$ is given by $\mathbb{B}_k \cup \mathbb{L}_{k-1}$, where $\mathbb{B}_k$ denotes the label space for objects born at time k (and is disjoint from $\mathbb{L}_{k-1}$) and we do not consider clutter targets in designing GLMB, thus, the label u is not introduced.

Suppose that there are N_k actual targets at time k, with label $\mathbf{x}_{k,1}, ..., \mathbf{x}_{k,N_k}$, in the context of multi-object tracking, $\mathbf{X}_k = \{\mathbf{x}_{k,1}, ..., \mathbf{x}_{k,N_k}\} \in \mathcal{F}(\mathbb{X} \times \mathbb{L}_k)$, where $\mathcal{F}(\mathbb{X} \times \mathbb{L}_k)$ denotes the space of finite subsets of $\mathbb{X} \times \mathbb{L}_k$. We denote cardinality (number of elements) of $\mathbf{X}$ by $|\mathbf{X}|$ and the set of labels of $\mathbf{X}$, $\{\ell : (x, \ell) \in \mathbf{X}\}$, by $\mathcal{L}_{\mathbf{X}}$. Note that since the label is unique, no two objects have the same label, i.e. $\delta_{|\mathbf{X}|}(|\mathcal{L}_{\mathbf{X}}|) = 1$. Hence $\Delta(\mathbf{X}) \triangleq \delta_{|\mathbf{X}|}(|\mathcal{L}_{\mathbf{X}}|$ is called the *distinct label indicator*.

In the GLMB the posterior density takes the form of a generalized labeled multi-Bernoulli

$$\pi_{k-1}(\mathbf{X}) = \Delta(\mathbf{X}) \sum_{c \in \mathbb{C}} \omega_{k-1}^{(c)}(\mathcal{L}_{\mathbf{X}}) \left[p_{k-1}^{(\xi)}\right]^{\mathbf{X}}. \tag{5}$$

Given the posterior multi-object density of the form (5), the predicted multi-object density to time k is given by

$$\pi_{k|k-1}(\mathbf{X}) = \Delta(\mathbf{X}) \sum_{c \in \mathbb{C}} \omega_{k|k-1}^{(c)}(\mathcal{L}_{\mathbf{X}}) \left[p_{k|k-1}^{(c)}\right]^{\mathbf{X}} \tag{6}$$

where

$$\omega_{k|k-1}^{(c)}(L) = w_{B,k}(L \cap \mathbb{B}_k)\omega_{S,k}^{(c)}(L \cap \mathbb{L}_{k-1}),$$
$$p_{k|k-1}^{(c)}(x, \ell) = 1_{\mathbb{L}_{k-1}}(\ell)p_{S,k}^{(c)}(x, \ell) + (1 - 1_{\mathbb{L}_{k-1}}(\ell))p_{B,k}(x, \ell),$$
$$p_{S,k}^{(c)}(x, \ell) = \frac{\left\langle p_{S,k-1}(\cdot,\ell) f_{k|k-1}(x|\cdot,\ell), p_{k-1}^{(c)}(\cdot,\ell)\right\rangle}{\eta_{S,k}^{(c)}(\ell)}, \;\; \eta_{S,k}^{(c)}(\ell) = \left\langle p_{S,k-1}(\cdot,\ell), p_{k-1}^{(c)}(\cdot,\ell)\right\rangle,$$
$$\omega_{S,k}^{(c)}(L) = [\eta_{S,k}^{(c)}]^L \sum_{I \subseteq \mathbb{L}_{k-1}} [q_S^{(c)}]^{I-L}\omega_{k-1}^{(c)}, \;\; q_S^{(c)}(\ell) = \left\langle 1 - p_{S,k-1}(\cdot,\ell), p_{k-1}^{(c)}(\cdot,\ell)\right\rangle,$$

where c is the index for track hypothesis, L is an instance of label set, I is track labels from previous time step.

Moreover, the updated multi-object density is given by

$$\pi_{k|k}(\mathbf{X}|Z_k) = \Delta(\mathbf{X}) \sum_{c\in\mathbb{C}} \sum_{\theta\in\Theta_k} \omega_{Z_k}^{(c,\theta)}(\mathcal{L}_{\mathbf{X}}) \left[p_{k|k}^{(c,\theta)}(\cdot|Z_k)\right]^{\mathbf{X}} \tag{7}$$

where Θ_k is the space of mappings $\theta : \mathbb{L}_k \to \{0, 1, ..., |Z_k|\}$, such that $\theta(i) = \theta(i') > 0$ implies $i = i'$, and

$$\begin{aligned}
&\omega_{Z_k}^{(c,\theta)}(L) \propto \delta_{\theta^{-1}(\{0:|Z_k|\})}(L)\omega_{k|k-1}^{(c)}(L)[\eta_{Z_k}^{(c,\theta)}]^L, \\
&p_{k|k}^{(c,\theta)}(x,\ell|Z_k) = \tfrac{p_{k|k-1}^{(c)}(x,\ell)\psi_{Z_k}(x,\ell;\theta)}{\eta_{Z_k}^{(c,\theta)}(\ell)}, \;\; \eta_{Z_k}^{(c,\theta)}(\ell) = \left\langle p_{k|k-1}^{(c)}(\cdot,\ell), \psi_{Z_k}(\cdot,\ell;\theta)\right\rangle, \\
&\psi_{Z_k}(x,\ell;\theta) = \delta_0(\theta(\ell))(1 - p_{D,k}(x,\ell)) + (1 - \delta_0(\theta(\ell)))\tfrac{p_{D,k}(x,\ell)g_k(z_{\theta(\ell)}|x,\ell)}{\kappa_k(z_{\theta(\ell)})}
\end{aligned}$$

where $\kappa_k \sim \lambda_c\mathcal{U}(\mathcal{Z})$ denotes the clutter density. λ_c is the clutter rate which is assumed to known as a prior.

3.3. Boosted Generalized labeled Multi-Bernoulli Filter

In this paper, we propose a new RFS filter called Boosted GLMB filter that is a principled combination of RMB filter [7] and GLMB filter [8]. The GLMB filter is used as a main tracker that produces track parameters. The one-step RMB filter is employed to adapt unknown clutter rate based on provided track parameters (position mean and covariance) and track existence probability of the GLMB filter from the previous time step. Then, the estimated clutter rate from the one-step RMB filter is fed into the GLMB filter for clutter model to boost accurate tracking results. Figure 1 represents the relation between the GLMB filter and one-step RMB filter.

As will be specified in the following section, we consider a linear Gaussian model, thus, the Boosted GLMB filter is implemented by using Kalman filters. Track parameters in this implementation is a set of Gaussian parameters, i.e., mean and covariance matrix that represent kinematic states of the object.

Once the tracker is initialized, state mean, covariance matrix and track existence probability are produced by the GLMB filter. In addition, the track existence probability $r^{(\ell)}$ is obtained by enumerating track hypothesis weights from the GLMB density

as

$$r^{(\ell)} = \sum_{\xi \in \Xi} \sum_{I \subseteq \mathbb{L}} 1_I(\ell) \omega^{(I,\xi)}, \tag{8}$$

where I and ξ are track labels and data association map from the previous time step and the calculated track existence probability $r^{(\ell)}$ is used as the initial values of track existence probability r in RMB prediction Eq. (3).

Then, the clutter rate is simply obtained by the EAP estimate of clutter target number as

$$\hat{\lambda_c} = \sum_{i=1}^{M_k} r_{0,k}^{(i)} p_{D,0,k} \tag{9}$$

where $r_{0,k}^{(i)}$ is the existence probability of clutter target introduced in the previous section, $p_{D,0,k}$ is the probability of detection for clutter targets.

4. Experimental results

In this section, two kinds of real-world experimental results are given. First, the proposed tracker is evaluated for visual multi-object tracking datasets [9], [10], [11] with unknown false measurement rate. Second, cell tracking in microscopy image data is illustrated. Tracking performance is enumerated with respect to the well-known performance metrics, in [5], [12].

4.1. Object motion and measurement models and basic parameters

Dynamic motion model: Individual object kinematics are described by a 4D state vector $x_k = [\, p_{x,k}, \dot{p}_{x,k}, p_{y,k}, \dot{p}_{y,k} \,]^{\mathrm{T}}$ of position and velocity, which follows a constant velocity model with T_s equal to the sampling period of the video data, and process noise is modeled as Gaussian $v_k \sim \mathcal{N}(v_k; 0, Q)$, where $\mathcal{N}(z; m, P)$ denotes a normal distribution with mean m and covariance P; $Q = \sigma_v^2 I_2$, I_2 is the 2×2 identity matrix, and $\sigma_v = 3$ pixels/frame is the noise standard deviation (set by considering the maximum speed of the object with regard to the frame rate). These values are determined by the maximum allowable object motion with respect to the image frame rate. Hence, the transition density

$$f_{1,k|k-1}(x_k|x_{k-1}) = \mathcal{N}(x_k; Fx_{k-1}, Q),$$

where

$$F = I_2 \otimes \begin{bmatrix} 1 & T_s \\ 0 & 1 \end{bmatrix}.$$

For clutter targets, the transition density $f_{0,k|k-1}$, is given as a random walk model to describe arbitrary motion [7].

Observation model: Assuming that the object state $x_k = [p_{x,k}\dot{p}_{x,k}, p_{y,k}\dot{p}_{y,k}]^T$ (x-, y- positions and velocities) is observed with additive Gaussian noise, the measurement likelihood function is given by $g_k(z_k|x_k) = \mathcal{N}(z_k; Hx_k, \Sigma)$, z_k is the response from designated detector; $H = [1\ \ 0\ \ 1\ \ 0]$, i,e., x-, y- position is observed by the detector, Σ is the covariance matrix of the observation noise.

4.2. People tracking in vision

For the evaluation in real-world data, we are interested in tracking of multiple pedestrians. In this experiment, we apply the ACF detector [13] for well-known datasets in computer vision, i.e., "S2.L1" from PETS'09 dataset [11], "TUD-Stadtmitte" from TUD dataset [9], and "Bahnhof" and "Sunnyday" from ETH dataset [10]. The number of targets varies in time due to births and deaths, and the measurement set includes target-originated detections and clutter. In our experiments, we use the low threshold for nonmaximum suppression so as to have less number of miss-detections but increased false alarms with time-varying rate. It is more realistic setting especially in ETH dataset that is recorded with frequent camera view changes. The Boosted GLMB is compared with the original GLMB (with fixed clutter rate) [8], and state-of-the-art online Bayesian multi-object tracker called RMOT [14]. Quantitative experiment results are summarized in Table 1 using well-known performance indexes given in [5]. In Table 1, Boosted GLMB shows superior performance compared to the GLMB in all indexes and compatible with the recent online tracker, RMOT. The proposed Boosted GLMB outperforms other trackers with respect to FPF where tracker is able to effectively reject clutters with estimated clutter rate. On the hand, inferior performance in Fragmentation and ID switches are observed compared to RMOT due to the simple motion model.

4.3. Cell migration analysis in microscopy image

The proposed algorithm is also tested with live-cell microscopy image data for cell migration analysis. The proposed GLMB tracking method is tested on a real stem cell migration sequence. The image sequence is recorded for 3 days, i.e., 4320 min and each image is taken in every 16 min.

Performance comparison is conducted with the state-of-the-art Multiple Hypothesis Tracker (MHT) [15]. The same motion and measurement models are used as in the first experiments and spot detection in [15] is applied for the fair comparison. As shown in Figure 2, the proposed GLMB provides reliable tracking results compared to the MHT. The MHT is tuned to obtain the best tracking results. The GLMB tracker produces significantly less false tracks and alleviate fragmented tracks because the tracker efficiently manages time-varying clutter information and keep confident tracks. Quantitatively, as can be seen in Table 2, time averaged OSPA distances [12] for both trackers verify that the Boosted GLMB shows reliable performance even when the clutter rate is unknown.

5. Conclusion

In this paper, we propose a new multi-object tracking algorithm for unknown clutter rate based on RFS filters that is free from clutter parameter tuning. The one-step RMB filter for clutter rate estimation and GLMB filters for trajectory estimation are coupled by exchanging parameters for robust online visual multi-object tracking. Experimental results via people and cell tracking datasets with state-of-the-art online trackers illustrate that the proposed multi-object tracker shows reliable performance. Interesting future research direction would be the extension of the tracking algorithm to adaptive survival probability and handling of missed-detections for further improvement.

Acknowledgement

This work was supported by the Australian Research Council through a research grant DP160104662.

References

References

[1] R. Mahler, Statistical Multisource-Multitarget Information Fusion, Artech House, Inc., Norwood, MA, USA, 2007.

[2] R. Mahler, B.-T. Vo, B.-N. Vo, Cphd filtering with unknown clutter rate and detection profile, IEEE Trans. Signal Processing 59 (8) (2011) 3497–3513.

[3] M. D. Breitenstein, F. Reichlin, B. Leibe, E. Koller-Meier, L. V. Gool, Online multiperson tracking-by-detection from a single, uncalibrated camera, IEEE Trans. Pattern Anal. Mach. Intell. 33 (9) (2011) 1820–1833.

[4] R. Hoseinnezhad, B.-N. Vo, B.-T. Vo, D. Suter, Visual tracking of numerous targets via multi-bernoulli filtering of image data, Pattern Recognition 45 (10) (2012) 3625–3635.

[5] C. H. Kuo, R. Nevatia, How does person identity recognition help multi-person tracking?, in: Proc. IEEE Conf. Comput. Vis. Pattern Recog., 2011, pp. 1217–1224.

[6] A. Milan, S. Roth, K. Schinlder, Continuous energy minimization for multitarget tracking, IEEE Trans. Pattern Anal. Mach. Intell. 36 (1) (2014) 58–72.

[7] B.-T., B.-N. Vo, R. Hoseinnezhad, Robust multi-bernoulli filtering, IEEE Jour. of Select. Topics in Signal Process. 7 (3) (2013) 399–409.

[8] B.-T. Vo, B.-N. Vo, Labeled random finite sets and multi-object conjugate priors, IEEE Trans. Signal Processing 61 (13) (2013) 3460–3475.

[9] M. Andriluka, S. Roth, B. Schiele, Monocular 3d pose estimation and tracking by detection, in: Proc. IEEE Conf. Comput. Vis. Pattern Recog., 2010, pp. 623–630.

[10] A. Ess, B. Leibe, K. Schindler, L. V. Gool, A mobile vision system for robust multi-person tracking, in: Proc. IEEE Conf. Comput. Vis. Pattern Recog., 2008, pp. 1–8.

Dataset	Method	Recall	Precision	FPF	GT	MT	PT	ML	Frag	IDS
PETS09-S2L1	Boosted GLMB	90.2 %	89.5 %	0.03	19	90 %	10 %	0.0 %	23	10
	GLMB [8]	82.6 %	81.4 %	0.16	19	82.7 %	17.3 %	0.0 %	23	12
	RMOT [14]	80.6 %	85.4 %	0.25	19	84.7 %	15.3 %	0.0 %	20	11
TUD-Stadtmitte	Boosted GLMB	83.4 %	85.6 %	0.10	10	80 %	20 %	0.0 %	12	16
	GLMB [8]	80.0 %	83.0 %	0.16	10	78.0 %	22.0 %	0.0 %	23	12
	RMOT [14]	82.9 %	86.6 %	0.19	10	80 %	20 %	0.0 %	10	16
ETH BAHNHOF and SUNNYDAY	Boosted GLMB	73.1 %	82.6 %	0.78	124	60.4 %	34.6 %	5.0 %	110	20
	GLMB [8]	71.5 %	76.3 %	0.88	124	58.7 %	27.4 %	13.9 %	112	40
	RMOT [14]	71.5 %	76.3 %	0.98	124	57.7 %	37.4 %	4.8 %	68	40

Table 1: Comparison with recent online trackers

Method	Average OSPA
Boosted GLMB	5
MHT [15]	8.5

Table 2: Comparison of averaged OSPA distance

[11] J. Ferryman, in: IEEE Workshop Performance Evaluation of Tracking and Surveillance, 2009.

[12] D. Schuhmacher, B.-T. Vo, B.-N. Vo, A consistent metric for performance evaluation of multi-object filters, IEEE Trans. Signal Processing 56 (8) (2008) 3447–3457.

[13] P. Dollár, Z. Tu, P. Perona, S. Belongie, Integral channel features, in: Proc. British Machine Vision Conference, 2009, pp. 91.1–91.11.

[14] J. H. Yoon, M. H. Yang, J. Lim, K.-J. Yoon, Bayesian multi-object tracking using motion context from multiple objects, in: IEEE Winter Conf. on App. Comput. Vis., 2015, pp. 33–40.

[15] N. Chenouard, I. Bloch, J.-C. O.-Marin, Multiple hypothesis tracking for cluttered biological image sequences, IEEE Trans. Pattern Anal. Mach. Intell. 35 (11) (2013) 2736–2750.

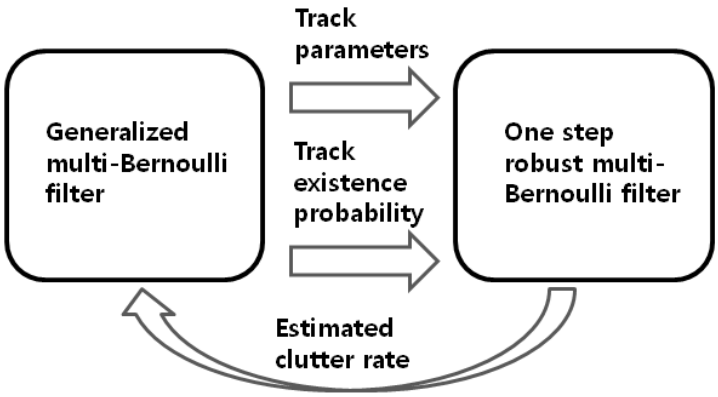

Figure 1: Schematic diagram of the Boosted GLMB

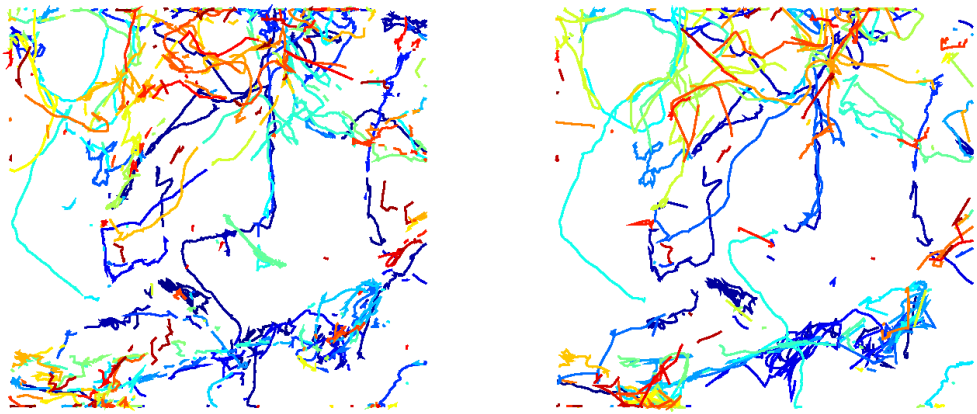

Figure 2: Reconstructed cell trajectories (left: MHT [15], right: Boosted GLMB)